AIP | Review of Scientific Instruments

Note: Velocity map imaging the scattering plane of gas surface collisions

D. J. Hadden, T. M. Messider, J. G. Leng, and S. J. Greaves

Citation: Review of Scientific Instruments **87**, 106104 (2016); doi: 10.1063/1.4965970

View online: http://dx.doi.org/10.1063/1.4965970

View Table of Contents: http://scitation.aip.org/content/aip/journal/rsi/87/10?ver=pdfcov

Published by the AIP Publishing

Note: Velocity map imaging the scattering plane of gas surface collisions

D. J. Hadden, T. M. Messider, J. G. Leng, and S. J. Greaves[a)]
Institute of Chemical Sciences, Heriot-Watt University, Edinburgh EH14 4AS, United Kingdom

(Received 13 June 2016; accepted 9 October 2016; published online 24 October 2016)

The ability of gas-surface dynamics studies to resolve the velocity distribution of the scattered species in the 2D scattering plane has been limited by technical capabilities and only a few different approaches have been explored in recent years. In comparison, gas-phase scattering studies have been transformed by the near ubiquitous use of velocity map imaging. We describe an innovative means of introducing a dielectric surface within the electric field of a typical velocity map imaging experiment. The retention of optimum velocity mapping conditions was validated by measurements of iodomethane-d_3 photodissociation and SIMION calculations. To demonstrate the system's capabilities, the velocity distributions of ammonia molecules scattered from a polytetrafluoroethylene surface have been measured for multiple product rotational states. [http://dx.doi.org/10.1063/1.4965970]

It has been noted by several authors[1–4] that the study of gas-surface scattering (SS) could be revolutionized by using a combination of resonance enhanced multiphoton ionization (REMPI)[5] and velocity map ion imaging (VMI).[6] REMPI-VMI allows the velocity distribution of quantum state selected products to be recorded; this approach has already been widely adopted in the gas-phase scattering community[7] as an improvement on previous techniques, e.g., traditional rotatable mass spectrometers,[8] which do not detect the 2D scattering plane in a single measurement.

VMI uses the interpenetrating electric fields generated by annular electrodes to map ions with the same velocity, but created in different locations, onto the same spot on a position sensitive detector.[6] Even small perturbations to these carefully created electric fields result in the loss of "velocity mapping" conditions, so approaches to imaging the scattering from surfaces have endeavored to minimize these effects by either mounting the surface onto an electrode,[2,3] or outside the electrodes altogether (see Ref. 1 and references therein). These approaches mean that it is no longer possible to image the whole 2D scattering plane, and so multiple measurements are still required to obtain the total scattering distribution.

Detecting the velocity distribution of the whole 2D scattering plane in a single measurement requires the scattering plane to be parallel to the position sensitive detector. If the surface is mounted onto one of the electrodes[3] then the scattering plane, which must contain the surface normal, is necessarily perpendicular to the detector preventing its direct measurement. Thus, either complex modeling or multiple time slicing measurements are required to deconvolute the velocity profile. Furthermore, only grazing angles of incidence are possible, as gas molecules have to pass between the electrodes to strike the surface.[3]

Experiments that mount the surface outside the electrodes[1] are limited to having a large surface to laser distance; this means that the ionization region has to be particularly large to avoid preselecting molecules and therefore biasing the measured distribution to a small range of scattering angles. This requires very shallow electric gradients that limit such techniques to only spatially imaging the scattered products and all velocity information has to be inferred from multiple images collected at individual time steps. In this paper, we present a novel adaptation to a standard VMI apparatus that overcomes these issues and provides a mechanism for directly imaging the scattering plane irrespective of the incident angle and should allow novel REMPI-VMI studies to be performed on numerous gas (dielectric) surface scattering systems.

The Surface-Scattering VMI (SS-VMI) experimental setup consisted of two differentially pumped chambers: a source chamber, that contained the molecular beam source; and a scattering chamber, which housed the laser focal region, the VMI electrodes (ion optics), the surface, and time-of-flight (TOF) region. The laser, TOF, and the molecular beam axes are mutually perpendicular (labeled x, y, and z, respectively, see Fig. 1) and meet at the center of the scattering chamber.

The molecular beam source consisted of a pulsed solenoid valve (General Valve, series 9) that was used to form a supersonic expansion of ammonia (2.5% in 4 bars He) or iodomethane-d_3 (2.5% in 4 bars Ar), with mean velocities of 1550 ms^{-1} and 540 ms^{-1}, respectively. The molecular beam was collimated by a 1.01 mm skimmer (Beam Dynamics, model 1) mounted at the intersection between the two chambers, 33 mm from the front face of the nozzle and 176 mm from the laser axis.

A pulsed dye laser (Sirah Cobra-Stretch, DCM dye) pumped by a Nd:YAG laser (Continuum Surelite, SL I-20) was used to generate all required laser light. The 2 mm diameter laser beam was focused into the center of the scattering chamber by a 250 mm focal length lens. The generated ions were accelerated by the ion optics electric field along a 500 mm field free TOF region until they reach a position sensitive detector (Photek VID240 and GM-MCP-2). Ion hits were recorded by a CCD camera (Basler scA780-54fm), with

a)Author to whom correspondence should be addressed. Electronic mail: s.j.greaves@hw.ac.uk.

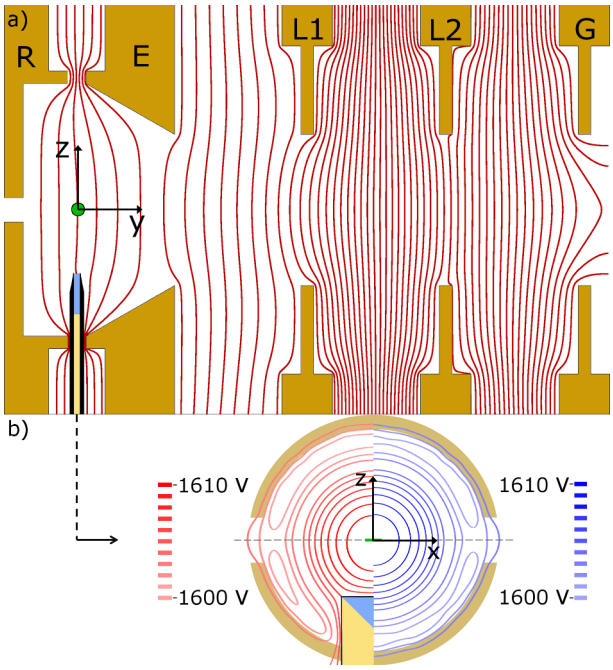

FIG. 1. (a) A cross section of the ion optics (orange), the surface and its mounting in the yz plane. The repeller, extractor, two lenses, and ground are labelled R, E, L1, L2, and G, respectively. The laser position is represented by the green dot. The red contours represent the SIMION calculated electric field and are spaced at 30 V intervals. (b) A perpendicular cross section in the xz plane, taken at the midpoint through the surface. The left side with red contours represents the imaging field in the presence of the polytetrafluoroethylene (PTFE) surface. The right side with the blue contours shows the field without the surface present. The green rectangle represents the ionization region. The PTFE section is shown in light blue, polyether ether ketone (PEEK) holder in yellow, and the scalpel blades are shown in black.

image acquisition and analysis performed by purpose written LabVIEW programs.

The ion optics (see Fig. 1) are based on those used by Livingstone *et al.* (shown in Fig. 4 of Ref. 9) and comprised five electrodes: a cup shaped repeller, a conical extractor, two additional annular lenses, and ground. Careful optimization of the ion optics' voltages and fast pulsing of the second MCP (40 ns temporal width) allowed for dc-slice imaging, where only the central "slice" of the ion packet was acquired.[10] This allowed the imaging of only those products in the scattering plane defined by the molecular beam and the surface (i.e., the xz plane).

The surface studied was Polytetrafluoroethylene (PTFE) with an exposed top face of 1 mm (y-axis) by 12.7 mm (x-axis) that was normal to the molecular beam direction (z-axis, with positive z defined as being away from the surface). The PTFE surface was mounted in a Polyether ether ketone (PEEK) holder of the same cross section, which extends approximately 50 mm down from the surface into a region outside the ion optics. Two stainless steel scalpel blades (A.C.M. 18) were attached to the long sides of the PEEK holder. These scalpel blades were employed as compensating electrodes to stabilize the electric field and maintain optimum velocity mapping conditions. Scalpel blades were used for these electrodes as their sharp edges produce minimal electric field perturbation, as well as having a narrow cross section to minimize undesired scattering. The PEEK holder was mounted in the scattering

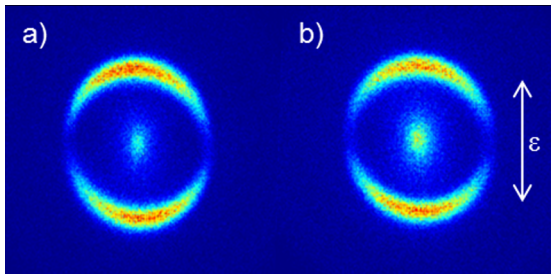

FIG. 2. (a) Velocity map image and (b) surface scattering velocity map image of iodine cations formed by one color photodissociation of iodomethane-d_3 as described in the text. The electric field polarization of the dissociation laser is noted by the double-ended white arrow in (b).

chamber via an XYZ translator, which allowed accurate positioning of the surface, or its removal from the electric field region to enable comparative measurements using the "standard" VMI technique (referred to as VMI mode from hereon). All SS-VMI experiments were performed with the PTFE surface held 10 mm from, and aligned centrally to, the x and y axes. Optimum electrode voltages were 1700, 1505, 1273, and 569 V for R, E, L1, and L2, respectively; with blade voltages of 1628 and 1598 V. The SIMION contours in Fig. 1 show that the surface causes only a minimal perturbation to the curvature of the field.

To compare the velocity mapping conditions of the experiment in VMI and SS-VMI modes, one color photodissociation of CD_3I and subsequent ionization of $I(^2P_{1/2})$ atoms were performed at 310.6 nm, using a (2 + 1) REMPI scheme.[11] Fig. 2 shows the resultant images, with Fig. 2(a) taken in VMI mode and Fig. 2(b) in SS-VMI mode. From a comparison of the images, it is clear that introducing the dielectric surface had minimal effect on the velocity mapping conditions (i.e., no surface charging effects were observed); the radii of the rings vary by less than a pixel. This negligible difference is also emphasized by the small change of detector slice timing required to obtain the center of the iodine ion packet: a 5 ns change on a 16.24 μs flight time (0.03%).

Images of surface scattered NH_3 were recorded in three different rotational states: $J_K = 1_0$, 5_3, and a combination of the $8_6/10_9$ levels in a single band; and are shown in Fig. 3. Ionization of scattered NH_3 molecules was by (2 + 1) REMPI.[5] The rotational levels studied were isolated spectroscopic transitions that represent low, medium, and high J_K cases in the scattered signal. Images in Fig. 3 were taken at a delay of 90 μs after the appearance of the molecular beam signal, which is ample time for scattered ammonia to make the 20 mm round-trip.

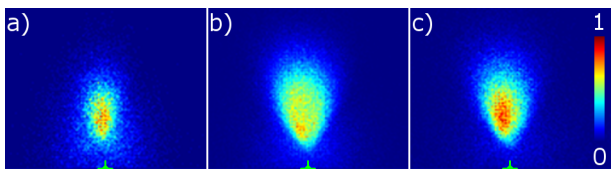

FIG. 3. Surface scattering velocity map images of ammonia cations formed from the J_K = (a) 1_0, (b) 5_3, and (c) $8_6/10_9$ rotational levels of the $\tilde{X}$ state. The green tick marks at the bottom of each image correspond to zero lab frame velocity.

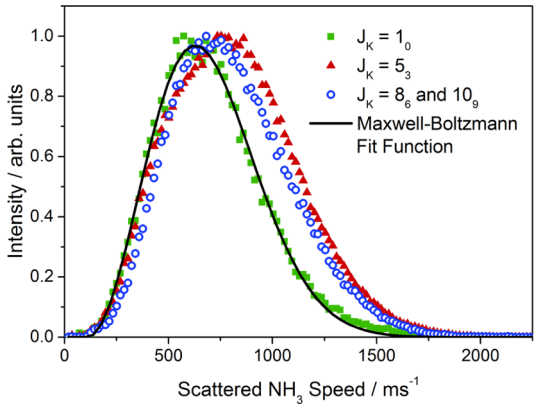

FIG. 4. Scattered ammonia speed distributions derived from Fig. 3, measured for the $J_K = 1_0$, 5_3, and $8_6/10_9$ rotational levels of the ammonia $\tilde{X}$ state. A Maxwell-Boltzmann distribution is fit to the $J_K = 1_0$ signal, with a mean ammonia velocity of 694 ms^{-1}.

It should be noted that the slight perturbation of the electric field, predicted by the SIMION calculations (Fig. 1), is far more significant for ions whose lab frame velocity is directed towards the surface (negative z), while ions with a lab frame velocity away from the surface (positive z) will experience minimal perturbation of the electric field. For the CD_3I images in Fig. 2(b), both the upper and lower crescents of the rings have negative z velocities in the lab frame. However, scattered NH_3 possess positive z velocity taking these ions away from the surface to an area where the electric field is unperturbed.

Speed distributions of the scattered NH_3 are obtained by radially integrating the signal in a 90° wedge centered on the positive z direction from zero lab frame velocity (ZLFV). Radial integration of 90° wedges perpendicular to the molecular beam (i.e., along the x-axis), from ZLFV, were used to obtain and subtract the background signal caused by NH_3 scattering from the chamber walls and electrodes. This background is visible in Fig. 3 close to ZLFV. The radial signal is then converted to speed by a calibration factor (17.92 ms^{-1} $pixel^{-1}$ for NH_3) determined from the CD_3I images. Normalized speed profiles of the scattering signal (from Fig. 3) are shown in Fig. 4. These profiles show that there is a large exchange of translational energy during the collision between NH_3 and surface. By fitting the speed profile to a Maxwell-Boltzmann distribution, a mean NH_3 speed[12] can be obtained (694 ms^{-1} for $J_K = 1_0$) that is significantly slower than the incoming molecular beam velocity. We note that the loss in translational energy does not follow a trend dependent on J, as the mean speed increases from $J_K = 1_0$ to 5_3 (821 ms^{-1}) and then decreases again from 5_3 to $8_6/10_9$ (799 ms^{-1}).

All scattered signal in Fig. 3 lies in a narrow range of angles (approximately 75° centered on positive z from the ZLFV). The angular distribution of signal shows only a slight change across the three rotational levels studied, with $J_K = 1_0$ showing a narrower spread by approximately 15°. It should be noted that the range of measurable scattering angles is currently limited by our detection geometry and Rayleigh range to 80°.

In conclusion, we have demonstrated the viability of SS-VMI as a means of directly detecting the 2D velocity distribution in the scattering plane of a gas-surface collision, which can lead to more rigorous studies of scattering dynamics. The calculations of electric field contours and the experimental iodomethane-d_3 photodissociation images have shown the feasibility of using stabilizing electrodes to maintain velocity mapping conditions while introducing a dielectric object (in this case the PTFE surface) inside the VMI ion optics. Ammonia scattering results have highlighted the quality of the velocity distributions that can be obtained with these experiments. Although the range of detectable scattering angles currently limits the technique, it is expected that an alternative ion optics design will allow a reduction of the surface to laser distance (while maintaining velocity mapping conditions). Coupled with greater laser Rayleigh range, this will minimize the level of background signal, improve velocity resolution, and allow a greater than 150° range of measurable angles.

S.J.G. thanks the EPSRC for a Career Acceleration Fellowship (Grant No. EP/J002534/2). T.M.M. is grateful to Heriot-Watt University for a Ph.D. studentship. We would like to thank Cassandra Rusher for experimental assistance; Professor Matt Costen and Professor Ken McKendrick for their helpful discussions and loan of experimental equipment.

[1]D. J. Harding, J. Neugebohren, D. J. Auerbach, T. N. Kitsopoulos, and A. M. Wodtke, J. Phys. Chem. A **119**, 12255 (2015).
[2]S. P. K. Koehler, Y. Y. Ji, D. J. Auerbach, and A. M. Wodtke, Phys. Chem. Chem. Phys. **11**, 7540 (2009).
[3]J. R. Roscioli and D. J. Nesbitt, Faraday Discuss. **150**, 471 (2011).
[4]M. Reid and S. P. K. Koehler, Rev. Sci. Instrum. **84**, 6 (2013).
[5]M. N. R. Ashfold, R. N. Dixon, N. Little, R. J. Stickland, and C. M. Western, J. Chem. Phys. **89**, 1754 (1988).
[6]A. Eppink and D. H. Parker, Rev. Sci. Instrum. **68**, 3477 (1997).
[7]G. R. Wu, W. Q. Zhang, H. L. Pan, Q. Shuai, B. Jiang, D. X. Dai, and X. M. Yang, Rev. Sci. Instrum. **79**, 094104 (2008).
[8]W. B. Miller, S. A. Safron, and D. R. Herschbach, Discuss. Faraday Soc. **44**, 108 (1967).
[9]R. A. Livingstone, J. O. F. Thompson, M. Iljina, R. J. Donaldson, B. J. Sussman, M. J. Paterson, and D. Townsend, J. Chem. Phys. **137**, 17 (2012).
[10]D. Townsend, M. P. Minitti, and A. G. Suits, Rev. Sci. Instrum. **74**, 2530 (2003).
[11]L. Minnhagen, Ark. Fys. **21**, 415 (1962).
[12]These speed distributions are likely a convolution of multiple factors, for this reason they are described in terms of mean speed rather than temperature. The Maxwell-Boltzmann fits yield mean speeds which correspond to characteristic temperatures of 276 K, 442 K, and 365 K for $J_K = 1_0$, 5_3, and $8_6/10_9$, respectively. Mean speed (S) is calculated from this temperature (T), molecular mass (m), Boltzmann constant (K_b), and offset (x_0) using $S = 2\sqrt{(2/\pi)} \times \sqrt{K_b T/m} + x_0$.